Investigating wear performance of surface treated additively manufactured Ti-6Al-4V temporomandibular joint replacement implants

Sizwe Ntimane[1*], *Gerrie* Booysen[2], and *Kobus* van der Walt[1]

[1]Central University of Technology Free State, Department of Mechanical and Mechatronic Engineering, 20 President Brand Street, Bloemfontein, South Africa
[2]Central University of Technology Free State, Centre for Rapid Prototyping and Manufacturing, 20 President Brand Street, Bloemfontein central, Bloemfontein, South Africa

Abstract. Severe damage to the Temporomandibular Joint (TMJ) may require surgical reconstruction through Total Joint Replacement (TJR) implants. These implants experience progressive tribological degradation over time, which ultimately necessitates revision surgery. Various surface treatments such as oxygen boost diffusion (OBD) and nitride heat treatment of titanium alloy components manufactured using Additive Manufacturing (AM) were investigated to improve wear properties. This study reports preliminary test results, with Pin-on-disc (POD) testing showing clear wear improvements in treated components.

1 Introduction

The temporomandibular joint (TMJ) is a bilateral joint that connects the mandible to the skull and gives the ability for mastication and speech. It is one of the joints in the human body that is used continually [1]. The mouth can be opened and closed as many as 2000 times a day, through articulation of the TMJ [2]. It is a unique and complex joint in the body because it has two condyles (bicondylar) functioning together, with the movement being concurrent due to the condyles being connected to the mandible at opposite sides. The TMJ is made up of three significant parts: the glenoid fossa, mandibular condyle, and mandibular ramus (Fig. 1). The TMJ is a synovial joint (joints found between bones that move against each other) with six degrees of freedom, including both rotation and translational movements [3].

* Sizwe Ntimane : sizwentimane@gmail.com

© The Authors, published by EDP Sciences. This is an open access article distributed under the terms of the Creative Commons Attribution License 4.0 (https://creativecommons.org/licenses/by/4.0/).

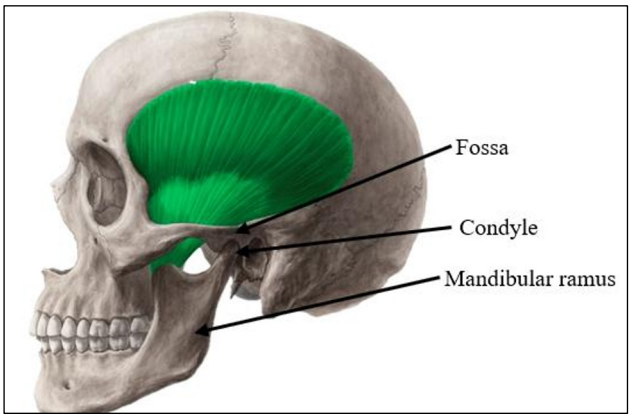

Fig. 1. The three components of the TMJ [32]

Various factors can lead to TMJ dysfunction, resulting in disorders such as disc displacement, dislocation, inflammation, ankylosis, and osteoarthritis [5]. These conditions often impair mastication and speech due to associated pain. In trauma patients, limited or even complete inability to open the mouth is common [4, 5]. Total joint replacement (TJR) surgery is considered a last-resort treatment option when other interventions fail to restore joint functionality [5, 6, 9].

A Temporomandibular joint replacement system comprises out of two components: a mandibular implant and a fossa prosthesis (Fig. 2) [7–9]. Commercial solutions are supplied either as stock or as patient-specific components. Although stock implants offer immediate availability, their standard geometry often yields sub-optimal bone contact and non-ideal screw positioning in anatomically complex mandibles [23–26]. Custom TJRs, designed from the patient's CT data, provide superior fit and optimised fixation but incur longer design–manufacture lead times and higher costs [23–26]. Historically, mandibular implants have been machined or cast from Cobalt–Chromium–Molybdenum (CoCrMo) or wrought Titanium Aluminium Vanadium (Ti-6Al-4V) alloys [9, 10]. This study is focused on mandibular implants fabricated from Ti-6Al-4V using Direct Metal Laser Sintering (DMLS), an Additive- Manufacturing (AM) process that enables patient-matched geometries and porous interfaces for osseointegration. The fossa component follows current clinical practice and is machined from Ultra-High-Molecular-Weight Polyethylene (UHMWPE) via precision Computer Numerical Control (CNC) milling [9, 10].

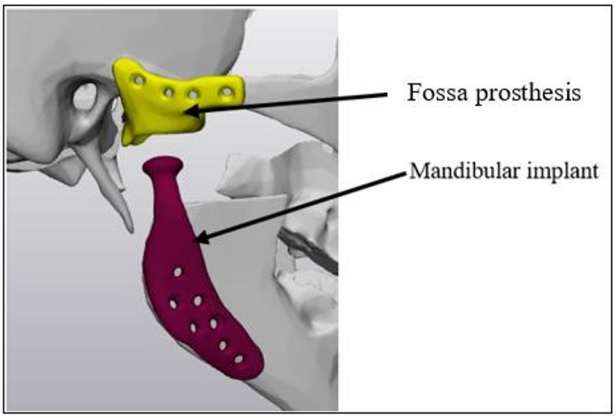

Fig. 2. Components of the TMJ replacement implant

Material wear resistance is a key factor influencing the longevity and functional success of TMJ replacement implants after implantation. Ti-6Al-4V elicits a favourable biological response, particularly osseointegration [11, 12], when compared to other metallic materials used in TJR implants. This response facilitates bone growth around or into the implant, depending on its surface characteristics and design features. However, the Ti-6Al-4V exhibits inferior wear properties compared to CoCrMo [13]. To enhance the wear resistance of Ti-6Al-4V, various surface treatment processes have been explored. Park et al. investigated plasma carburising of Ti-6Al-4V and reported enhanced wear properties due to the formation of a coating layer approximately 150 µm thick [15]. Cremer et al. examined oxide layer formation during Oxygen Boost Diffusion (OBD) of Ti-6Al-4V and found that the characteristics of the oxide layer varied with the thermal treatment employed [16]. Similarly, Lee et al. studied nitride coating formation at β-phase temperatures (around 950°C), reporting a ~40 µm thick nitride layer [17]. Other studies have demonstrated that similar nitride coatings can be achieved at lower temperatures using extended holding times. For example, Khatru et al. observed that increasing both temperature and holding time enhances the mean hardness of the material [18].

2 Methods and materials

The tribological behaviour of the treated samples was evaluated using the Pin-On-Disc (POD) method, with Ti-6Al-4V serving as the pin (representing the mandibular implant) and cross-linked UHMWPE (representing the fossa prosthesis) as the disc material. Tests were performed under lubricated conditions using bovine serum, which mimics the tribological environment of the TMJ, as validated by Hembus et al. [19]. This makes it a suitable lubricant for in vitro wear testing of TMJ related materials. The experimental procedure will follow American Society for Testing and Material (ASTM) G99, the standard method for conducting POD tests. Test parameters were guided by the methodology described by Zdero et al. [20], with additional insights from studies by Van Loon et al. [21] and Xiong et al. [22]. Furthermore, relevant elements from ASTM F732 and ASTM F1714 were incorporated to support the design and interpretation of the wear testing. The aim of this study was to investigate the wear performance of Ti-6Al-4V mandibular implants manufactured using DMLS subjected to two surface modification techniques: Nitrite Heat Treatment (NHT) and OBD.

2.1 Sample fabrication

The materials used in this study included Ti-6Al-4V pin specimens fabricated through the DMLS AM process. The specimens were produced on an Electro-Optical System (EOS) M290 machine under standard process parameters, utilising Ti-6Al-4V Grade 23 powder produced by EOS. Post-manufacturing, the pins were subjected to stress relief (SR) heat treatment at 650°C for 3 hours and annealing (AN) heat treatment at 940°C for a 2-hour cycle under controlled conditions in the T-M Vacuum Products Inc. SS12/24-13MDX vacuum furnace to reduce residual stresses and enhance microstructural stability. The UHMWPE discs were manufactured using CNC machining. The material was crosslinked with an irradiation dose of 76 kGy, which is known to influence wear resistance. In accordance with ASTM G99 standards, the pins were designed with a spherical geometry and a diameter of 6 mm, while the discs measured 30 mm in diameter and 5 mm in thickness. Tribological testing was performed under lubricated conditions, employing bovine serum as the lubricant. Following the procedures specified in ASTM F732 and ASTM F1714, the bovine serum solution was prepared by dissolving 20 g/l of bovine serum, 7.44 g/l of ethylenediaminetetraacetic acid (EDTA), and 1.85 g/l of sodium azide in deionised water, to

a total volume of 500 ml. The solution was stirred continuously for 15 minutes to ensure adequate mixing.

The Ti-6Al-4V pins were initially fabricated with an oversize of 2 mm to allow for post-processing through CNC machining aimed at enhancing surface finish. Surface roughness measurements in the radial direction yielded an average arithmetic roughness (R_a) of 0.434 µm, which complies with the surface roughness requirements specified in the ASTM G99 standard for POD wear testing. To further refine the surface, the pins underwent additional polishing using a GPAINNOVA Dlyte 100 H electropolishing machine, resulting in an improved R_a value of 0.175 µm. The CNC machined UHMWPE discs initially exhibited an average R_a of 1.099 µm. Hand polishing was performed using 400 grit followed by 1000 grit abrasive paper, which improved the surface roughness to 0.254 µm.

2.2 Surface treatment process

A total of nine Ti-6Al-4V pins were subjected to the final polishing step using the Dlyte 100 H electropolishing machine, after which they all displayed a uniform, reflective silver appearance. Of these, three pins underwent nitride heat treatment, three underwent oxygen boost diffusion (OBD), and the remaining three were retained as untreated controls.

2.2.1 Nitride heat treatment (NHT)

The specimens designated for nitride heat treatment were subjected to a surface process aimed at forming a hard titanium nitride (TiN) layer The treatment was carried out in the T-M Vacuum Products Inc. SS12/24- 13MDX vacuum furnace at a constant temperature of 850 °C for a duration of5 hours. During this time, nitrogen gas was introduced into the furnace chamber to promote the diffusion of nitrogen into the titanium substrate and facilitate TiN formation. Upon completion of the treatment cycle, the pins were allowed to cool under vacuum conditions to prevent oxidation and preserve surface integrity.

2.2.2 Oxygen boost diffusion (OBD)

The specimens designated for oxygen boost diffusion (OBD) treatment were processed to investigate the effect of oxygen diffusion on surface wear resistance. The OBD method employed in this study was adapted from the procedure described by Cremer et al. [16] and consists of a distinct three-stage process. In the first stage, the pins were placed in the Nabertherm LH 120/12 furnace under ambient air conditions and heated to 680 °C for 16 hours. This oxidation step allowed for the enrichment of oxygen at the surface, resulting in the formation of a thin oxide layer. The furnace was then allowed to cool gradually to room temperature.

In the second stage, the oxidised pins were transferred to the T-M Vacuum Products Inc. SS12/24-13MDX vacuum furnace, where the temperature was increased to 850 °C. The pins were held at this temperature for 5 hours under vacuum to facilitate the inward diffusion of oxygen atoms into the titanium microstructure. This stage promoted the development of a hardened oxygen diffusion zone below the surface without the formation of a separate coating.

In the final stage, the pins were reintroduced into the Nabertherm LH 120/12 furnace and again subjected to 680 °C for 16 hours. After the heat- cycle, the furnace was allowed to cool to room temperature under ambient conditions. Visual inspection revealed the presence of residual oxide on the pin surfaces, which appeared as oxide grain clusters formed during the thermal oxidation stage, consistent with previous reports. These clusters contributed to the

coarse surface finish observed. To address this, the pins were subsequently buffed using a polishing wheel to remove the oxide residue and restore a smoother surface.

2.3 Experimental set-up

Wear testing was conducted using the POD Anton Paar Tribometer TRB3 (Fig. 3) in accordance with ASTM G99, under lubricated conditions designed to simulate the synovial environment of the TMJ. The experimental setup included the Ti-6Al-4V pins both untreated (only SR and AN heat treatment) and surface-treated (via NHT and OBD) mounted vertically and loaded with a 10N mass against cross-linked UHMWPE discs mounted on a rotating platform (Fig. 4). Prior to wear testing, the Ti-6Al-4V samples were cleaned using propanol and handled with nitrile gloves to prevent contamination. The UHMWPE samples were cleaned with ethanol using wipes and allowed to air-dry at room temperature before mounting. The system is equipped with an integrated profilometer, which traverses the wear track to measure its depth. These measurements, combined with test parameters such as pin radius, applied load, sliding speed, and number of cycles, are used to calculate wear volume, from which the wear rate is determined.

Fig. 3. Pin-on-disc tribometer (TRB3) employed for wear testing.

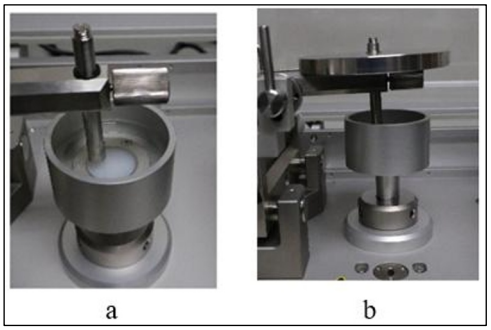

Fig. 4. Experimental setup showing the UHMWPE disc and Ti-6Al-4V pin assembly. (a) UHMWPE disc is mounted in a rotating cup, (b) Normal load applied to the Ti-6Al-4V pin during testing

The test parameters were selected based on established tribological studies related to joint implants [20–22] and included the following conditions: sliding speed of 0.05 m/s and 500000 cycles. The rotation radius was maintained at 8 mm from the centre of the disc, resulting in a circular wear path on the UHMWPE disc. While many tribological studies

employ linear sliding motion, the current investigation was constrained by the experimental setup, which permitted only rotational motion under lubricated conditions. Each test was run for approximately 5 days and 20 hours to complete the required number of cycles. All experiments were conducted at room temperature (28 ± 2 °C).

Lubrication was provided using a prepared bovine serum solution, as described in Section 2.1. The UHMWPE disc and Ti-6Al-4V pin were immersed in the lubricant for ~5 hours prior to testing to ensure consistent fluid-film lubrication throughout the test duration. To maintain the integrity of the serum and minimise protein degradation or microbial growth, fresh serum was used for each test cycle and replaced at 250000 cycles. After each lubricant replacement, the rotating cup was cleaned with deionised water before adding fresh bovine serum to minimise biofilm formation and maintain consistent testing conditions. Bovine serum is commonly used as a synovial fluid analogue in wear testing due to its protein content and similarity to joint fluid, which helps replicate physiological lubrication [33]

Following completion of the wear tests, the wear rate of the cross-linked UHMWPE discs was evaluated using the Surtronic® S-100 series profilometer which is integrated with the POD Tribometer TRB3. Measurements were taken at three distinct locations on each disc, and the average value was calculated to represent the wear rate.

2.4 Surface characterisation

Surface characterisation was conducted on the Ti-6Al-4V pins to evaluate the effects of the surface treatments (NHT and OBD). Surface morphology was examined at University of the Free State (UFS) using the Joel JSM 6610 scanning electron microscope (SEM) operated at 20 kV. SEM images were captured at various magnifications to observe surface features, the wear track, and potential delamination. Elemental analysis was performed using Energy-Dispersive X-ray Spectroscopy (EDS), integrated with the SEM system, to confirm the incorporation of nitrogen and oxygen into the respective surface-treated pins.

The Ti-6Al-4V pin specimens were mounted in thermoplastic resin using a Struers CitoPress-1 hot compression mounting press to facilitate precise sectioning. Each sample was positioned in a mounting mould with phenolic resin powder, then subjected to a temperature of approximately 180 °C and a pressure of ~3 bar for 10 minutes. After cooling under pressure, the solidified mounts were removed and grinded using a Struers Tegramin 25 system until the central axis of the pins was exposed; samples were then etched to reveal their microstructural features. SEM imaging was then used to analyse the treated layer and evaluate the layer formed due to the surface treatments.

Surface roughness of the Ti-6Al-4V pins was measured along the radial direction at eNtsa (Nelson Mandela University in Gqeberha, South Africa) using a Mitutoyo SURFTEST SJ-210 (Model ENT15015). Ra values were recorded at three different locations per sample, and the mean value was reported. For the UHMWPE discs, surface roughness was measured using a Surtronic® S-100 series profilometer. Ra values were obtained from three distinct areas on each disc, and the average value was reported.

3 Results and discussion

3.1 Results

3.1.1 Surface roughness

Surface roughness measurements (R_a) before and after treatment are summarized in Table 2. The Untreated (SR & AN) pins exhibited the lowest roughness (R_a = 0.175 μm), while nitride

treated pins showed a moderate increase due to nitride layer formation (R_a = 0.318 µm). The OBD treated pins showed a higher increase in the surface roughness in comparison to the nitride treated pins, measuring 0.346 µm R_a after the full treatment cycle. The UHMWPE measured 0.254 µm R_a after hand polishing using abrasive paper.

Table 2. Measured surface roughness of Ti-6Al-4V pins and UHMWPE discs following surface treatment and polishing.

Surface roughness (R_a in µm)		
	Finishing process	**Arithmetic roughness**
Ti-6Al-4V pins	Post Dlyte polishing (Control group)	0.175 µm
	Post NHT	0.318 µm
	Post OBD surface treatment	0.346 µm
UHMWPE discs	Post hand polishing using abrasive paper	0.254 µm

3.1.2 Surface appearance and morphology

Visual inspection showed clear differences in the surface coloration after each heat treatment process on the Ti-6Al-4V pins. The untreated (SN & AN) pin displayed a mirror-like finish indicating a smooth and polished surface (Fig. 5 A). Post NHT, the surface of the pins turned into a golden colour and a reduced mirror-like reflective finish. The colouring was consistent throughout the surface of the part showing a uniform layer formation of the nitride (Fig. 5 B). OBD treated Ti-6Al-4V pins showed a brown coloration after the initial oxidation stage which reverted to a mirror-like finish after heat treatment under vacuum and finally developed a bronze like colour following the final oxidation stage (Fig. 5 C).

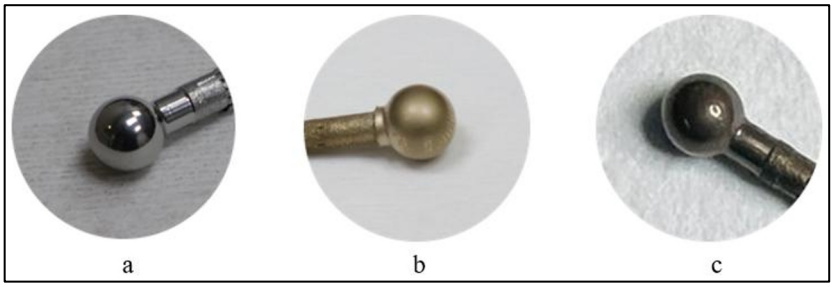

Fig. 5. Ti-6Al-4V pins before and after surface treatment. (a) Untreated Ti-6Al4V pin, (b) Nitride treated Ti-6Al4V pin, (c) OBD treated Ti-6Al4V pin.

SEM analysis of the untreated Ti-6Al-4V pin, following final polishing, revealed a smooth and uniform surface morphology characterized by well-defined concentric polishing marks (Fig. 6a). These features are indicative of consistent rotary polishing and confirm the achievement of a uniform surface finish. No surface defects such as microcracks, delamination, or surface contamination were detected, and the absence of any secondary surface features confirms that the specimen remained in its as-polished state without prior surface modification. The surface roughness (Ra) for this condition was measured at

0.255 µm, serving as a baseline reference for comparison with surface heat-treated counterparts.

SEM examination of the OBD-treated Ti-6Al-4V pin, following the final oxidation stage and subsequent mechanical polishing, also displayed a smooth and continuous surface (Fig. 6b). Swirled polishing patterns were observed, indicating effective mechanical removal of the thin surface oxide formed during the final thermal oxidation step. The surface showed no signs of cracking, delamination, or morphological defects, suggesting that the OBD process followed by polishing successfully preserved the structural and morphological integrity of the near-surface region.

In contrast, SEM imaging of the NHT Ti-6Al-4V pin surface revealed a distinct matte and moderately textured morphology, markedly different from the untreated and OBD-treated samples (Fig. 6c). The surface exhibited fine, speckled microstructural features and shallow topographical irregularities, which are consistent with the formation of a TiN compound layer. Although faint polishing lines were still discernible, their subdued appearance indicates that the nitriding process significantly modified the surface topography. No cracking or delamination was observed, implying a uniform, adherent TiN layer. These morphological characteristics align with the increased surface roughness measured for the NHT Ti-6Al-4V pin and support the presence of a hard, wear-resistant surface layer formed via nitrogen diffusion.

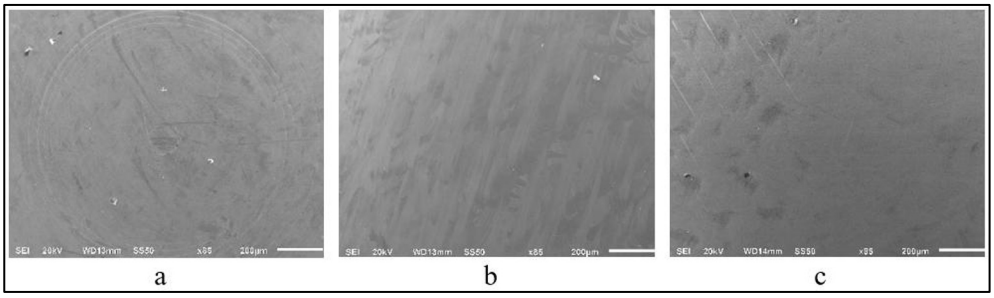

Fig. 6 Surface SEM images of Ti-6Al-4V pins before wear test. (a) Untreated pin, (b) OBD treated pin, (c) NHT pin

3.1.3 Phase composition

EDS analysis of the untreated and OBD-treated Ti-6Al-4V pins prior to wear testing revealed similar elemental surface compositions at the outermost surface (Fig. 7a, 7b). While EDS did not detect a strong oxygen signal, it should be noted that EDS has limitations in quantifying light elements, and a surface oxide layer may still be present, as indicated by the brown coloration of the OBD-treated pins. Long oxidation steps, as employed in this study, can result in multi-layered oxides such as Al_2O_3 and TiO_2. This observation aligns with the expected outcome of the OBD process, which enhances surface hardness through subsurface oxygen diffusion. Cremer et al. reported that OBD processing can produce surface oxide layers approximately 2–4 µm thick, which may be partially removed by light polishing, supporting the interpretation of subsurface oxygen enrichment in the present results. EDS point scans for the NHT Ti-6Al-4V pin revealed elevated nitrogen concentrations on the surface, consistent with the formation of a TiN layer (Fig. 7c).

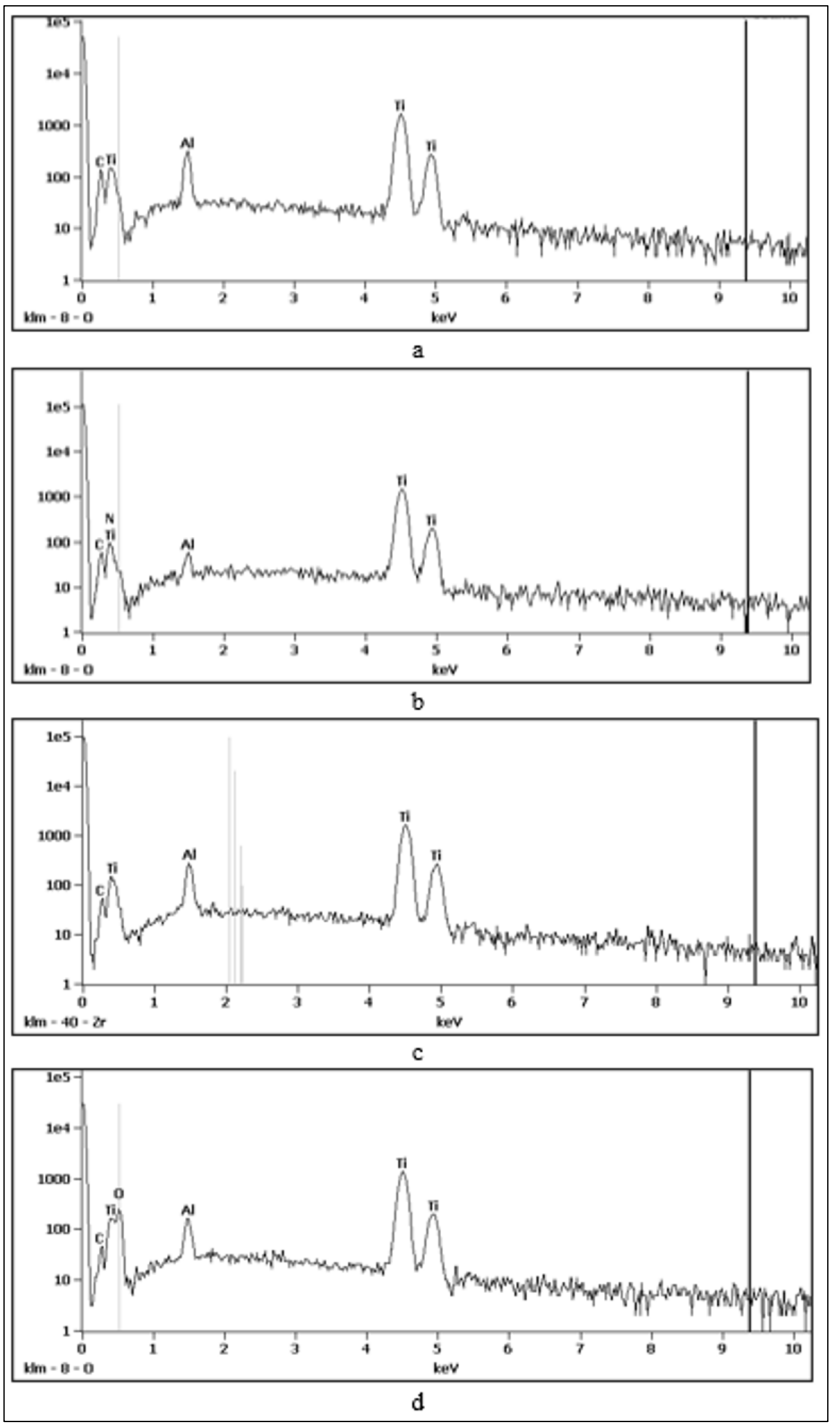

Fig. 7. EDS scans showing the elemental analysis of the surface treated Ti-6Al-4V pins. (a) Untreated pin (b) NHT pin (c) OBD treated Ti-6Al-4V pin, (d) Sectioned OBD treated Ti-6Al-4V pin

The Ti-6Al-4V pins were sectioned (Fig. 8) and SEM images were taken to examine the effects of the surface treatments. In the OBD-treated pin, a light region just beneath the

surface was observed (Fig. 9a). While this was initially interpreted as oxygen diffusion into the material without a visible surface coating, it is acknowledged that such features may also arise as a sample preparation artefact. Specifically, incomplete planarization during polishing can result in rounding at the edges due to the higher hardness of the oxide layer, which may give the appearance of a uniform subsurface zone. Nevertheless, EDS point analysis confirmed increased oxygen concentrations within this region (Fig. 7d), supporting the interpretation of oxygen enrichment associated with the OBD process. The NHT pin showed a clear surface layer (Fig. 9b), likely made of titanium nitride (TiN), with a zone beneath it where nitrogen had diffused into the metal. This surface layer appeared even and strongly bonded to the base material. The untreated sample displayed a typical α+β structure with no surface changes, serving as the reference for comparison. These images confirm that both OBD and nitriding changed the near-surface structure of the alloy in ways that are likely to improve hardness and wear resistance.

Fig. 8 Sectioned Ti-6Al-4V pins, showing printing orientation on the Z direction.

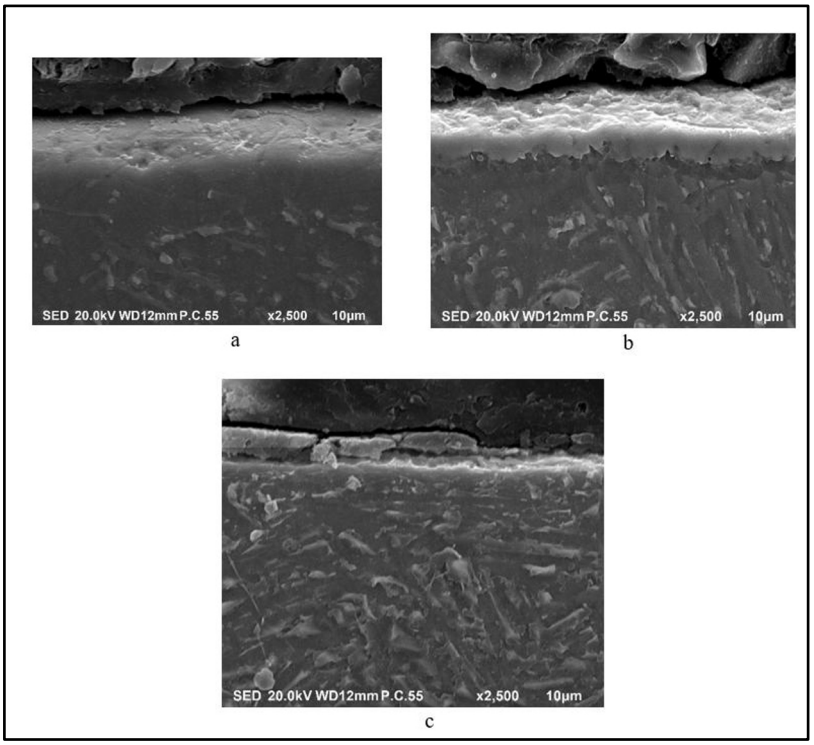

Fig. 9. SEM images of sectioned pins, (a, OBD treated pin (b) NHT pin, (C)Untreated pin

3.1.4 Wear rate analysis

Wear rates for the untreated, NHT, and OBD Ti-6Al-4V pins were evaluated using the POD method under lubricated conditions with bovine serum, in accordance with ASTM G99, ASTM F732 and ASTM F1714. The wear results are primarily evaluated based on the wear of the UHMWPE disc, as it serves as the softer articulating counterpart in the metal-on-polymer pairing and is therefore expected to exhibit the most significant material loss. The wear performance was assessed by measuring the wear rate using the Surtronic® S-100 series which is incorporated with the Tribometer TRB3. Quantitatively, the NHT pin exhibited the lowest wear rate of 1.059×10^{-6} mm³/N.m, followed by the OBD treated pin, and lastly the untreated pin with the highest wear rate. The findings indicate that both surface treatments effectively enhance the wear resistance of Ti-6Al-4V, with the nitriding process exhibiting the greatest improvement, likely due to the formation of a hard, wear-resistant TiN surface layer. Table 3 shows the summary of the wear results

Table 3. Summary of the wear performance of the experiment.

Test load	Number of cycles	Pin	Disc	Wear rate
10N	500 000	Ti-6Al-4V untreated	UHMWPE cross-linked	$1.682 \times 10^{-6}\text{mm}^3/\text{N.m}$
10N	500 000	Ti-6Al-4V NHT	UHMWPE cross-linked	$1.059 \times 10^{-6}\text{mm}^3/\text{N.m}$
10N	500 000	Ti-6Al-4V OBD treated	UHMWPE cross-linked	$1.456 \times 10^{-6}\text{mm}^3/\text{N.m}$

3.2 Discussion

This study evaluated the wear performance of Ti-6Al-4V pins versus UHMWPE cross-linked discs using a pin-on-disc wear test method under lubricated conditions simulating the TMJ. The Ti-6Al-4V pins underwent surface treatment through nitriding and OBD. The aim was to assess how these surface modifications influence tribological behaviour, particularly for medical implants used in TMJ reconstruction.

3.2.1 Surface morphology

Surface roughness increased following both treatments (from 0.175 µm to 0.318 µm for NHT and 0.346 µm for OBD-treated pins). Despite this increase, wear resistance improved, highlighting that enhanced hardness and surface chemistry play a more critical role in tribological performance than surface roughness alone. The relatively low wear rates of UHMWPE against surface-treated Ti-6Al-4V pins further confirm improved tribological compatibility. These results support previous observations by Shi et al. [28], who noted that engineered oxide surfaces reduce UHMWPE wear by minimising polymer transfer.

SEM surface analysis highlighted the morphological changes resulting from each treatment. The untreated (SR and AN) pin displayed a smooth and uniform surface with well-defined concentric polishing marks and no evidence of surface modification. This sample served as the baseline condition. The OBD treated pin maintained a smooth appearance, with visible rotary polishing patterns and no evidence of delamination, cracking, or surface degradation. These findings suggest that the treatment preserved the surface integrity while achieving subsurface hardening. In contrast, the NHT pin showed a more textured, matte surface morphology with speckled features and reduced visibility of polishing lines. These characteristics, along with the EDS confirmation of nitrogen enrichment, support the

formation of a hard TiN surface layer. The absence of surface defects also indicates that the nitride layer was uniformly formed and well-adhered to the base material.

3.2.2 Phase composition

The NHT Ti-6Al-4V pin exhibited a hardened surface layer, likely corresponding to the formation of a titanium nitride (TiN) compound. SEM cross-sectional imaging revealed a distinct surface layer with a moderately textured and matte appearance. These features are consistent with the formation of a TiN or Ti_2N compound layer, supported by EDS analysis which confirmed elevated nitrogen concentrations at the surface. This observation aligns with findings by Goratouch et al. [27], who reported the formation of compound layers consisting of Ti_2N and δ-TiN phases after plasma nitriding of Ti-6Al-4V, with increased layer thickness and intensity under higher nitriding temperatures and longer durations. The presence of a continuous, well-adhered compound layer in this study further supports the effectiveness of the nitriding process in creating a hard, wear-resistant surface

The OBD process followed the methodology described by Cremer et al. [16] and produced microstructural changes typical of solid-state diffusion treatments. The OBD process followed the methodology described by Cremer et al. [16] and produced microstructural changes typical of solid-state diffusion treatments. The treated pin exhibited a subsurface oxygen diffusion zone (ODZ) with a gradual transition into the bulk material. While no distinct compound layer was observed in the present analysis, literature indicates that the third step of OBD promotes the growth of an adherent oxide layer on top of the ODZ. The absence of a retained surface oxide in the current observations may be related to the specimen preparation and polishing procedure for metallographic analysis. EDS analysis revealed the absence of detectable oxygen at the outermost surface, which is attributed to the mechanical polishing step performed after the final oxidation stage. This step may have reduced or thinned the oxide film, which is typically around 2–4 μm in thickness as reported by Cremer et al. for OBD-treated Ti-6Al-4V. However, EDS point analysis within the subsurface region confirmed elevated oxygen levels, verifying the formation of the ODZ even though no distinct oxide layer was detected in the current measurements. It is recognised that an adherent oxide layer is expected from the OBD process, and its absence here may reflect preparation artefacts rather than a deviation from the underlying mechanism.

3.2.3 Wear performance

The wear test results demonstrated that both surface treatments significantly enhanced the tribological performance of Ti-6Al-4V when tested against cross-linked UHMWPE. The untreated pin exhibited the highest wear rate at 1.682×10^{-6} mm³/N·m, serving as the baseline for comparison. NHT resulted in the most substantial improvement, reducing the wear rate to 1.059×10^{-6} mm³/N·m. This improvement is attributed to the formation of a hard TiN surface layer, which enhances surface hardness and reduces material loss during articulation. These findings are consistent with literature reports, including those by Shi et al. [28], who observed improved wear resistance following surface oxidation treatments, as well as other studies highlighting the tribological benefits of TiN-coated Ti-6Al-4V [30, 31].

The OBD-treated pin also showed improved wear resistance compared to the untreated sample, with a wear rate of 1.456×10^{-6} mm³/N·m. Although no surface compound layer was present, the oxygen diffusion zone (ODZ) formed during treatment likely contributed to increased subsurface hardness. This mechanism aligns with previous findings [28–31], which show that surface hardening through diffusion whether via nitrogen or oxygen can effectively reduce wear, though performance gains depend on treatment depth, uniformity, and surface preparation.

4 Conclusion

This study investigated the tribological performance of Ti-6Al-4V subjected to two surface treatment techniques NHT and OBD using a pin-on-disc wear testing protocol under lubricated conditions simulating the TMJ environment.

4.1 Key findings

- NHT led to the most significant reduction in wear rate, attributed to the formation of a continuous and well-adhered TiN compound layer, as confirmed by SEM and EDS analysis.

- OBD treatment also enhanced wear resistance by introducing a subsurface oxygen diffusion zone (ODZ), improving hardness without forming a brittle surface layer or compound coating offering a potentially more stable alternative to coated surfaces

- Untreated (SR and AN) Ti-6Al-4V demonstrated the highest wear rate, reaffirming the alloy's limitations in its raw state and the importance of surface modification for biomedical load-bearing applications.

- Surface roughness, morphology, and phase composition analyses verified that both surface treatments were successfully applied. The observed microstructural changes corresponded to improvements in wear resistance and support the distinct mechanisms of each treatment.

4.2 Future work

These findings highlight the importance of surface engineering in extending the functional lifespan of Ti-6Al-4V components in TMJ replacement implants. Ongoing work involves extended wear testing up to 5×10^6 cycles to assess long-term durability. Future studies will include micro-indentation hardness profiling to correlate mechanical gradients with diffusion depth, advanced cross-sectional characterisation of treated zones, and in vitro biocompatibility evaluations to assess clinical relevance. Additional investigations will focus on optimizing post-treatment polishing techniques to preserve the surface oxide layer in OBD treated pins and evaluating wear behaviour when the OBD cycle is stopped after the vacuum diffusion stage, potentially reducing processing time while retaining surface benefits.

References

1. A. Ramos, M. Mesnard, Christensen vs Biomet Microfixation alloplastic TMJ implant: Are there improvements? A numerical study J. Craniomaxillofac. Surg, **43,** 1384-1391 (2015)
2. S. Ingawalé, T. Goswami, Temporomandibular joint: Disorders, treatments, and biomechanics, Ann. Biomed. Eng, **37,** 976-996 (2009)
3. C. Norkin, P. Levangie, Joint Structure & Function: A Comprehensive Analysis, 193-205 (F.A. Davis Coompany, Philadelphia, 1992)
4. H. Mohammad, A Textbook of Advanced Oral and Maxillofacial Surgery, **3**, 560–576 (IntechOpen, Chicago, 2016)

5. D. Ackland, D. Robinson, M. Redhead, P. Vee Sin Lee, A. Moskaljuk, G. Dimitroulis, A personalized 3D-printed prosthetic joint replacement for the human temporomandibular joint: From implant design to implantation, J. Mech. Biomed. Mater, **69**, 404-411 (2017)
6. L. Wolford, P. Mehra, Custom-Made Total Joint Prostheses for Temporomandibular Joint Reconstruction, Proc (Bayl Univ Med Cent), **13**, 135-138 (2000)
7. Z. Afzal, M. Umorin, L.G. Mercuri, G. Warburton, TMJ Concepts Patient-Fitted Temporomandibular Joint Reconstruction Prosthesis System: Results from an FDA Post-Market Surveillance Prospective Cohort Study, J. Oral Maxillofac. Surg, 83, 10-16 (2025)
8. A. Westmark, P. Heden, E. Aagaard, C. Cornelius, The use of TMJ Concepts prostheses to reconstruct patients with major temporomandibular joint and mandibular defects, Int. J. Oral Maxillofac. Surg, **40**, 487-496 (2011)
9. N. Meurechy, A. Braem, M. Mommaerts, Biomaterials in temporomandibular joint replacement: current status and future perspectives – a narrative review, Int. J. Oral Maxillofac. Surg, **47**, 518-533 (2018)
10. S. Huys, D. Alonso, P. Theuns, G. van Lenthe, J. Sloten, M. Mommaerts, A novel 3D-printed, patient-specific alloplastic temporomandibular joint replacement allowing enthesis reconstruction: A finite element analysis, Ann. 3D Print. Med, **6** (2022)
11. S. Rastegari, E. Salahinejad, Surface modification of Ti-6Al-4V alloy for osseointegration by alkaline treatment and chitosan-matrix glass-reinforced nanocomposite coating, Carbohydr. Polym, **205**, 302-311 (2019)
12. G. Sovak, I. Gotman, A. Weiss, Osseointegration of Ti–6Al–4V Alloy Implants with a Titanium Nitride Coating Produced by a PIRAC Nitriding Technique: A Long-Term Time Course Study in the Rat, Microsc. Microanal, **21,** 179-189 (2015)
13. E. Atar, Sliding wear performances of 316 L, Ti6Al4V, and CoCrMo alloys, J. Met. Mater, **51**, 183-188 (2013)
14. D. Royhman, J. Yuan, T. Shokuhfar, C. Takoudis, C. Sukotjo, M. Mathew, Tribocorrosive behaviour of commonly used temporomandibular implants in a synovial fluid-like environment: Ti-6Al-4V and CoCrMo, J. Phys. D: Appl. Phys, **46** (2013)
15. Y. Park, M. Wey, S. Hong, Enhanced wear and fatigue properties of Ti-6Al-4V alloy modified by plasma carburizing/CrN coating, J. Mater. Sci. Mater. Med, **18**, 925-931 (2007)
16. L. Cremer, J. van der Merwe, T. Becker, Oxygen boost diffusion of additively manufactured Ti-6Al-4V for improved oxide layer adhesion, J. Alloys Compd, **1031**, (2025)
17. D. Lee, W. Abro, K. Lee, M. Abro, I. Pohrelyuk, O. Yaskiv, Gas Nitriding and oxidation of Ti-6Al-4V alloy, DDF, **382**, 155-159 (2018)
18. R. Khatru, R. Singh, Surface Treatment of Ti-6Al-4V by Nitriding Heat Treatment Process, Int. J. Curr. Eng. Technol, **04**, 2833-2836 (2014)
19. J. Hembus, P. Henke, J. Hellwig, A. Klinder, R. Bader, Experimental analysis of the wear behavior of total knee endoprostheses with bovine serum and synthetic synovial fluid as lubricants, Tribol. Int, **195** (2024)
20. R. Zdero, L. Guenther, T. Gascoyne, Pin-on-Disk Wear Testing of Biomaterials Used for Total Joint Replacements, in Experimental methods in orthopaedic biomechanics, Academic Press, 299-311 (2016)

21. J. van Loon, G. Verkerke, M. de Vries, L. de Bont, Design and Wear Testing of a Temporomandibular Joint Prosthesis Articulation, J Dent Res, **79**, 715-721 (2000)
22. D. Xiong, Z. Gao, Z. Jin, Friction and wear properties of UHMWPE against ion implanted titanium alloy, Surf Coat Tech, **201**, 6847-6850 (2007)
23. H. Liu, L. Huang, S. Liu, L. Liu, B. Li, Z. Zheng, Y. Liu, X. Liu, E. Luo, Evolution of temporomandibular joint reconstruction: from autologous tissue transplantation to alloplastic joint replacement, Int. J. Oral Sci, **17** (2025)
24. S. Kanatsios, A. Thamos, S. Tocaciu, Comparative clinical outcomes between stock vs custom temporomandibular total joint replacement systems, J. Craniomaxillofac. Surg, **50**, 322-327 (2022)
25. Z. Brown, S. Sarrami, D. Perez, Will they fit? Determinants of the adaptability of stock TMJ prostheses where custom TMJ prostheses were utilized, Int. J. Oral Maxillofac. Surg, **50**, 220-226 (2021)
26. N. De Meurechy, C. Zaror, M. Mommaerts, Total Temporomandibular Joint Replacement: Stick to Stock or Optimization by Customization?, CMTR, **13**, 59-70 (2020)
27. G. Ongtrakulkij, J. Kajornchaiyakul, K. Kondoh, A. Khantachawana, Investigation of Microstructure, Residual Stress, and Hardness of Ti-6Al-4V after Plasma Nitriding Process with Different Times and Temperatures, Coatings, **12** (2022)
28. S. Wen, D. Han-shan, Improvement in the Tribological Properties of UHMWPE Sliding against Ti6AI4V by Surface Modification, J. Shanghai Univ, **9**, 164-171 (2005)
29. E. Atar, Sliding wear performances of 316 L, Ti6Al4V, and CoCrMo alloys, Kovove Mater, **51**, 183-188 (2013)
30. H. Man, M. Bai, F. Cheng, Laser diffusion nitriding of Ti-6Al-4V for improving hardness and wear resistance, Appl. Surf. Sci, **258**, 436-441 (2011)
31. O. Tkachuk, S. Sheykin, S. Lavrys, I. Yu Rostotskii, M. Danyliak, Effect of stage gas nitriding on corrosion and wear resistance of Ti6Al4V alloy in physiological environment, Vacuum, **230** (2024)
32. Ken hub | https://www.kenhub.com/en/library/anatomy/the-skull-joints, Accessed: 23 April 2025
33. M. Wimmer, R. Sah, M. Laurent, A. Virdi, The effect of bacterial contamination of friction and wear in metal/polyethylene bearings for total joint repair-A case study, Wear, **301**, 264-270 (2013)